certain perturbations, the open-loop model is unstable. For this reason it cannot be used to model high frequency uncertainty.

Acknowledgment

The author would like to thank J. Fanson, J. Garba, and C.-C. Chu of the Jet Propulsion Laboratory for their help and encouragement. An anonymous reviewer suggested that an extension to real perturbations (Section III-B) was possible. This suggestion, and the other comments, are appreciated.

References

[1] B. G. Morton and R. M. McAfoos, "A mu-test for robustness analysis of a real-parameter variation problem," in *Proc. Amer. Contr. Conf.*, 1985.

[2] R. S. Smith, "Modeling real parameter variations in flexible structures with complex valued perturbations," in *Proc. IEEE Conf. Decis. Contr.*, 1991, pp. 1638–1639.

[3] R. S. Smith, C-C. Chu, and J. L. Fanson, "The design of H_∞ controllers for an experimental noncollocated flexible structure problem," *IEEE Trans. Contr. Syst. Tech.*, vol. 2, no. 2, pp. 101–109, June 1994.

[4] *μ-Analysis and Synthesis Toolbox (μ-Tools).* Natick, MA: The MathWorks, 1991.

[5] G. W. Stewart, *Introduction to Matrix Computations.* New York: Academic, 1973.

[6] R. A. Horn and C. R. Johnson, *Matrix Analysis.* Cambridge, England: Cambridge Univ. Press, 1985.

[7] G. J. Balas and J. C. Doyle, "Identification of flexible structures for robust control," *IEEE Contr. Sys. Mag.*, vol. 10, no. 4, pp. 51–58, June 1990.

Stability Margin Optimization via Interpolation and Conformal Mappings

Juan C. Cockburn, Yariv Sidar, and Allen R. Tannenbaum

***Abstract*— Many interesting problems of robust stabilization can be solved using the complex function theoretic approach of [1]. This method is based on the construction of a conformal mapping which reduces the original robust stabilization problem to a Nevanlinna–Pick interpolation problem. The main difficulty of this approach lies in the construction the conformal mapping. Here we present a new numerical algorithm to construct such conformal mappings. Then we demonstrate its effectiveness in the synthesis of optimal gain-phase margin controllers.**

I. Introduction

Many problems of robust stabilization and sensitivity minimization can be studied using classical complex function theory and conformal mappings [2], [1]. The basic idea is to reduce them to an interpolation problem of the Nevanlinna–Pick type via conformal mappings. This method has been successfully applied to solve many interesting robust stabilization problems (e.g., see [3]–[5] and references therein). It has been limited, however, to applications where the conformal mapping can be found in closed form. In fact, the main difficulty with this approach is precisely the construction of such conformal maps. In this note we present a new numerical algorithm [6] that can be used effectively to construct such conformal mappings. The algorithm that we present here was developed by Marshall and Morrow (M&M) to study the generation of curves with prescribed harmonic measures and is based on elementary conformal mappings. For other applications of numerical conformal mapping to control problems, see [7]. This paper is organized as follows: in Section II we discuss the problem of robust stabilization of certain class of linear time-invariant (LTI) systems and present a short review of the function theoretic approach of [1]. In Section III we present the main result of this paper, namely, a detailed description of the new conformal mapping algorithm. In Section IV we discuss the gain-phase margin problem, which is one of the simplest robust stabilization problem for which no closed form for the conformal mapping is known. In Section V we use the new algorithm to solve the gain-phase margin problem. Finally in Section VI we draw some general conclusions. Our notation is standard; $\mathbf{C}$ denotes the complex plane and $\mathcal{RH}^\infty$ the set of real rational proper stable transfer functions. $\mathbf{D}, \mathbf{H}$, and $\mathbf{C}_+$ denote the open unit disk, open right-half plane, and open upper-half plane, respectively, and $\bar{\mathbf{H}} := \{s \in \mathbf{C} : \mathrm{Re}\, s \geq 0\} \cup \{\infty\}$ is the extended closed right-half plane.

Manuscript received December 8, 1993; revised May 4, 1994. This work was supported in part by National Science Foundation Grants DMS-8811084 and ECS-9122106, Air Force Office of Scientific Research Grants AFOSR-90-0024 and AF/F49620-94-1-00S80EF, and Army Research Office Grants DAAL03-91-G-0019, DAAH04-93-G-0332, and DAAH04-94-G-0054.

J. C. Cockburn is with the Institute for Mathematics and its Applications, University of Minnesota, Minneapolis, MN 55455-0436 USA.

Y. Sidear is with the Department of Electrical Engineering, Technion, Haifa, Israel 32000.

A. R. Tannenbaum is with the Department of Electrical Engineering, University of Minnesota, Minneapolis, MN 55455 USA.

IEEE Log Number 9409691.

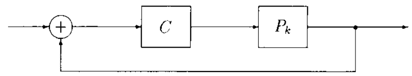

Fig. 1. A standard unity feedback system.

II. Robust Stabilization Problems and Interpolation

Consider the standard unity feedback system of Fig. 1 where P_k is a given parameterized family of scalar, LTI plants, k is a parameter vector taking values in some compact uncertainty set $\mathbf{K}$, and $C(s)$ the controller to be designed. We identify an arbitrary element $P_o(s) \in P_k$ as the nominal plant. Let $P_o(s)$ have nonminimum-phase zeros $\{\zeta_i \in \bar{\mathbf{H}} : i = 1, \cdots, n_\zeta\}$ and unstable poles $\{\pi_j \in \bar{\mathbf{H}} : j = 1, \cdots, n_\pi\}$. Furthermore, assume that all the plants $P(s) \in P_k$ have the same number of unstable poles. The general stability margin optimization problem can be stated as follows: Given a family of LTI plants P_k, design a (real rational proper) controller $C(s)$ such that for every $k \in \mathbf{K}$ the closed-loop system is internally stable and certain stability margin is maximized. Here stability margin is any suitable measure of the "size" of the smallest perturbation $k \in \mathbf{K}$ that destabilizes the system and the optimal controller will be the one that maximizes the size of the perturbation k among all stabilizing controllers. In its full generality the above problem is still open. In many problems of practical interest, however, the uncertainty set $\mathbf{K} \subset \mathbf{C}$ can be modeled as a simply connected domain, and it can be reduced to an interpolation problem via conformal mappings [1]. Let $S = [I + PC]^{-1}, P \in P_k$ denote the usual sensitivity function with S_o corresponding to the nominal plant P_o. To establish the relation between stability and interpolation consider the problem of nominal stabilization, e.g., $P_k = \{P_o\}$. Then we have the following theorem.

$$\begin{tikzcd} \tilde{\mathbf{H}} \arrow[rr, "S_o"] \arrow[dr, "\tilde{S}_o"'] & & \mathbf{G} \arrow[dl, "\theta"] \\ & \mathbf{D} & \end{tikzcd}$$

Fig. 2. Commutative diagram.

Theorem 1 (Nominal Stability [8]): The nominal unity feedback system is internally stable iff

a) $1 + P_o(s)C(s) \neq 0$ for all $s \in \tilde{\mathbf{H}}$.
b) There are no pole-zero cancellations in $\tilde{\mathbf{H}}$ when the product $P_o(s)C(s)$ is formed.

The above theorem implies that nominal stability is equivalent to a Lagrange interpolation problem: Find a real-rational, proper, analytic function $S_o : \tilde{\mathbf{H}} \to \mathbf{C}$ such that i) the zeros of $S_o(s)$contain $\{\pi_j\}_1^{n_\pi}$ and ii) the zeros of $S_o(s) - 1$ contain $\{\zeta_i\}_1^{n_\zeta}$. Note that a) in Theorem 1 imposes the analyticity condition on S_o while b) gives rise to the interpolation conditions. This interpolation problem is always solvable, and it is the presence of uncertainty that makes this stabilization problem nontrivial. To see this, consider the family of plants

$$P_k = kP_o(s) : k \in \mathbf{K} \subset \mathbf{C} \text{ simply connected }, \{0, \infty\} \not\subset \mathbf{K}\}.$$

From condition a) in Theorem 1 we have that $1+PC \neq 0, \forall P \in P_k$, $\forall s \in \tilde{\mathbf{H}}$ iff $[1 + P_oC][k - (k-1)S_o] \neq 0, \forall k \in \mathbf{K}$, $\forall s \in \tilde{\mathbf{H}}$. Equivalently $1 + P_o(s)C(s) \neq 0, \forall s \in \tilde{\mathbf{H}}$ and

$$S_o(s) \neq \frac{k}{k-1}, \forall k \in \mathbf{K}, \forall s \in \tilde{\mathbf{H}}. \tag{1}$$

This last equation means that $S_o : \tilde{\mathbf{H}} \to \mathbf{G}$, where $\mathbf{G} := \mathbf{C}\backslash\{k/(k-1) : k \in \mathbf{K}\}$. The conformal mapping $\phi_S : \mathbf{C} \setminus \mathbf{K} \to \mathbf{G}$ given by $\phi_S(z) = z/(z-1)$, induced by S, establishes the relation between the uncertainty, $\mathbf{K}$, and the range of S_o, $\mathbf{G}$.

Remark 1: We can as well formulate the stabilization problem in terms of the complementary sensitivity $T = 1 - S$. In that case, the reader can verify that the mapping from $\mathbf{C} \setminus \mathbf{K}$ to $\mathbf{G}$ is $\phi_T(z) = 1/(1-z)$.

The application of condition b) in Theorem 1 to P_k together with (1) lead to the following formulation of the stabilization problem.

Problem 1 (General Stability Margin Problem [1]): Given $\mathbf{G}$ a simply connected domain, with $\{0, 1\} \subset \mathbf{G}$. Find a function $S_o \in \mathcal{RH}^\infty$ such that the interpolation conditions are satisfied and $S_o : \tilde{\mathbf{H}} \to \mathbf{G}$. To reduce the general stability margin problem to an Nevanlinna–Pick interpolation problem we construct a conformal mapping $\theta : \mathbf{G} \to \mathbf{D}$ as shown in Fig. 2. The existence of this mapping is guaranteed by the Riemann Mapping Theorem (see Section III). Once we have constructed θ, we can obtain $S_o = \theta^{-1} \circ \tilde{S}_o$, where $\tilde{S}_o$ is the solution to the following Nevanlinna–Pick problem: Find a function $\tilde{S}_o \in \mathcal{RH}^\infty$ such that

$$\begin{array}{ll} i) & \text{the zeros of } \tilde{S}_o(s) - \theta(0) \text{ contain } \{\pi_j\}_1^{n_\pi} \\ ii) & \text{the zeros of } \tilde{S}_o(s) - \theta(1) \text{ contain } \{\zeta_i\}_1^{n_\zeta} \\ iii) & \|\tilde{S}_o\|_\infty < 1. \end{array} \tag{2}$$

The commutative diagram indicates that if there exists $\tilde{S}_o \in \mathcal{RH}^\infty$ that solves the above interpolation problem, then $S_o = \theta^{-1} \circ \tilde{S}_o$ solves the general stability margin problem.

Remark 2: The conformal mapping θ can be made unique by choosing $\theta(0) = 0$ and $\theta(1)$ a positive real. There is no guarantee that $S_o = \theta^{-1} \circ \tilde{S}_o$ be real-rational. If θ is real, however, e.g., $\overline{\theta(\bar{z})} = \theta(z)$, then so is S_o. The rationality of S_o is handled by standard approximation procedures [9]. Necessary and sufficient conditions for the solution of the general stability margin problem are given by the following theorem of [1]

Theorem 2: The general stability margin problem is solvable iff $|\theta(1)| < \alpha_{opt}$, where

$$\alpha_{opt}^{-1} := \inf_{C \text{ stabilizing}} \|S_o\|_\infty. \tag{3}$$

The key steps in the solution of problem 1 are: 1) the computation of the invariant α_{opt}, which only depends on the nonminimum phase zeros and unstable poles of $P_o(s)$ and 2) the computation of $|\theta(1)|$, which depends only on the uncertainty set $\mathbf{K}$ and requires the construction of the conformal mapping $\theta : \mathbf{G} \to \mathbf{D}$. In this paper we address the problem of constructing the mapping θ. The computation of α_{opt} is a standard problem in Nevanlinna–Pick theory.

III. Construction of the Conformal Equivalence: New Algorithm

Conformal mappings are essentially analytic functions with analytic inverse. The existence of such mappings between simply connected domains is a consequence of the classical Riemann Mapping Theorem [10] which says that any simply connected domain $\mathbf{G} \subset \mathbf{C}$, which is not the whole complex plane, can be conformally mapped onto the open unit disk $\mathbf{D}$. Such conformal mappings are called Riemann mappings. This theorem is an existence result, and its proofs are not constructive. Since in general it is not possible to find a closed form expression for such Riemann mappings, a practical approach is to devise computational algorithms to approximate these mappings. (In the sequel, domain refers to a simply connected domain that is not the whole complex plane.)

Suppose that $\theta : \mathbf{G} \to \mathbf{D}$ is the Riemann mapping, from a given domain $\mathbf{G}$ to the disk, that we want to approximate. There are two classical approaches to construct numerical approximations to θ: 1) osculation methods and 2) Schwarz–Christoffel transformations. Osculation methods generate a sequence of functions $\{f_k\}_1^n$ such that as $n \to \infty$, $\theta_n := f_n \circ f_{n-1} \circ \cdots \circ f_1 \to \theta$. Unfortunately, these methods suffer from slow convergence [11]. The Schwarz–Christoffel transformations (SCT) are based on an integral representation of the Riemann mapping from a polygonal domain to the canonical domain. In practice, methods based on the SCT are limited to polygonal regions with a few sides (no more than 20) [12]. In the context of robust stabilization, $\mathbf{G}$ will be a region bounded by Jordan arcs. The new algorithm that we present here can handle, without difficulty, arbitrary bounded regions approximated by hundreds of straight line segments. To illustrate the basic idea of the M&M algorithm, consider the upper half plane $\mathbf{C}_+$ with a polygonal slit (a cut) described by the straight segments joining $0, \gamma e^{i\pi a}, w_1, \cdots, w_4$ as shown in Fig 3. We want to map this slit onto the real line. The cornerstone of the M&M algorithm is the map $f : \mathbf{C}_+ \to \mathbf{C}_+$

$$w = f(z) = (z-a)^a (z+1-a)^{1-a} \quad : \quad a \in (0, 1) \tag{4}$$

which takes the points a and $a-1$ in the z−plane to the origin of the w−plane and the origin of the z−plane to the point $\gamma\, e^{i\pi a}$, with $\gamma \in (1/2, 1)$ as illustrated in Fig. 3.

This mapping "zips" the real line segments $[a-1, 0]$ and $[0, a]$ into a straight segment of length γ at an angle πa and maps $\mathbf{C}_+$ onto itself. Of primary interest for us is the inverse map $z = f^{-1}(w)$. We can see that $f^{-1} : \mathbf{C}_+ \to \mathbf{C}_+$ "unzips" the straight segment back into the real line. Applying this mapping consecutively for each straight segment in the slit, with appropriate parameter a, we will be able to pull back the slit onto the real line. A clever combination of the unzipping maps, linear fractional transformations, and other

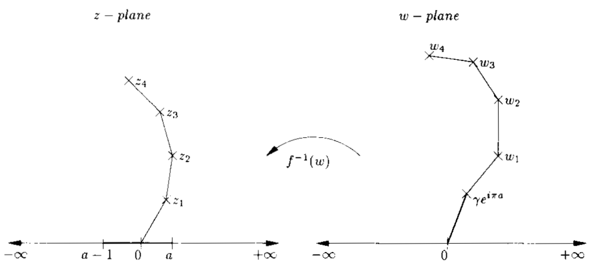

Fig. 3. "Unzipping" action of mapping $z = f^{-1}(w)$.

elementary mappings will allow us to construct the desired conformal mapping.

Let $\partial\mathbf{G}$, the boundary of $\mathbf{G}$, be described by a set of N points, $w_1, w_2, \cdots, w_N$, numbered counter-clockwise, with N even. Furthermore, assume that "kinks" can only occur at odd indexed points, except at the first point w_1. The M&M algorithm proceeds as follows.

M&M Algorithm: Input: $\{w_i\}_1^N \subset \partial\mathbf{G}$; *Output:* θ.

1) Map the complement of the circular arc through w_1, w_2, w_3 to the upper-half plane.
2) "Unzip" the curve from w_3 to w_{N-1} onto the real axis.
3) Map the remaining circular sector to the open unit disk.

To describe the details of the M&M algorithm we need to introduce some notation. Given a set of points $\{w_i\}_1^N \subset \partial\mathbf{G}$, denote by $w_k^{(i)}$ the image of the kth point w_k after a sequence of conformal transformations $\psi_i \circ \cdots \circ \psi_0$.

Step 1: Approximate the original curve segment between w_1 and w_3 with a circular arc and map the complement of this arc to $\mathbf{C}_+$. This can be accomplished by

$$\psi_0(w) = j\sqrt{\alpha_0 \frac{w - w_3}{w - w_1}} \quad ; \quad \alpha_0 = \frac{w_1 - w_2}{w_2 - w_3}. \tag{5}$$

After this mapping, the points $w_1^{(0)}, \cdots, w_3^{(0)}$ will lie on the real axis and $w_4^{(0)}, \cdots, w_N^{(0)}$ on $\mathbf{C}_+$.

Step 2: Pull the curve from $w_3^{(0)}$ to $w_{N-1}^{(0)}$, onto the real axis. To do this, first approximate the curve through $w_{3+2i}^{(i)}, w_{4+2i}^{(i)}, w_{5+2i}^{(i)}$ with a circular arc and map it to a straight segment with $w_{3+2i}^{(i)}$ as a fixed point (note that $w_{3+2i}^{(i)} = 0$) using

$$g_i^{-1}(w) = c_i \frac{w}{w - b_i} \tag{6}$$

$$b_i = \frac{Im\{1/\overline{w}_{4+2i}^{(i)} + 1/w_{5+2i}^{(i)}\}}{Im\{1/\overline{w}_{4+2i}^{(i)} 1/w_{5+2i}^{(i)}\}},$$

$$c_i = \gamma_i \frac{|w_{5+2i}^{(i)} - b_i|}{|w_{5+2i}^{(i)}|} < 1 \quad , \quad \gamma_i = a_i^{a_i}(1 - a_i)^{1-a_i}. \tag{7}$$

Then map this straight segment (through the points 0, $g^{-1}(w_{4+2i}^{(i)})$, and $g^{-1}(w_{5+2i}^{(i)})$) onto the real axis via $f_i^{-1}(w)$, where

$$f_i(w) = (w - a_i)^{a_i}(w + 1 - a_i)^{1-a_i} \quad ; \quad a_i \in (0, 1). \tag{8}$$

The composition of the two above maps, $\psi_i = f_i^{-1} \circ g_i^{-1}$ completes the ith iteration. This procedure is repeated $N/2$-2 times until all the points from w_{N-3} to w_{N-1} have been pulled onto the real line. (Note that at the i^{th} iteration we must have $w_{0+2i}^{(i)}, \cdots, w_{2+2i}^{(i)}$ all real, $w_{3+2i}^{(i)} = 0$ and $w_{4+2i}^{(i)}, \cdots, w_N^{(i)}$ all on $\mathbf{C}_+$.)

Step 3: Map the semi-infinite circular sector formed by $w_1^{(N/2-2)}, w_{N-1}^{(N/2-2)}$, and $w_N^{(N/2-2)}$, onto $\mathbf{D}$. To do this first map the circular sector to $\mathbf{C}_+$ using

$$p(w) = \left(\alpha_1 \frac{w}{\beta_1 - w}\right)^{\pi/\theta_1} \tag{9}$$

$$\alpha_1 = \frac{w_1^{(N/2-2)} - w_N^{(N/2-2)}}{w_N^{(N/2-2)}};$$

$$\beta_1 = w_1^{(N/2-2)}; \quad \theta_1 = Arg(w_1^{(N/2-2)^{-1}} - w_N^{(N/2-2)^{-1}}). \tag{10}$$

Finally, map $\mathbf{C}_+$ onto $\mathbf{D}$ via

$$q(s) = e^{i\theta_2}\frac{s - \beta_2}{s - \overline{\beta}_2} \tag{11}$$

$$\beta_2 = \Psi(0) \quad , \quad \theta_2 = -Arg(\Psi(1)) \tag{12}$$

where $\Psi = p \circ \psi_{N/2-2} \circ \cdots \circ \psi_0$. This particular choice of θ_2 and β_2 ensures that $\theta(0) = 0$ and $\theta(1)$ is positive real. The mapping $\psi_{N/2-1} = q \circ p$ completes the construction.

The approximate Riemann mapping, $\theta : \mathbf{G} \to \mathbf{D}$, is given by the composition of the $N/2$ elementary maps $\theta = \psi_{N/2-1} \circ \psi_{N/2-2} \circ \cdots \circ \psi_0$. It is characterized by the parameters (w_1, w_2, w_3), $\{(a_i, b_i, c_i)\}_1^{N/2-2}$, and $(\alpha_1, \beta_1, \beta_2, \theta_1, \theta_2)$. The computation of these parameters takes approximately $\mathcal{O}(N^2)$, an order of magnitude less than SCT methods. (An interesting problem would be a precise analysis of the sensitivity of the algorithm to the number of points $w_1, \cdots, w_N$. To the best of our knowledge such analysis has not been realized yet.)

Once we have found the parameters, the forward map $\theta : \mathbf{G} \to \mathbf{D}$ can be evaluated. The only transformations that cannot be obtained explicitly are the functions $\{f_i^{-1}(z)\}_1^{N/2-2}$ which must be computed numerically. This can be done by solving the nonlinear equation $v = f_i(w)$, v fixed using any appropriate numerical method. In particular, if we use Newton's method, we will have

$$w^{(k+1)} = w^{(k)} - \frac{f_i(w^{(k)}) - v}{f_i'(w^{(k)})}. \tag{13}$$

To guarantee the convergence of (13) we choose $w^{(0)}$ appropriately according to the location of the point v with respect to the straight segment from zero to $\gamma_i e^{j\pi a_i}$.

The computation of the inverse map $\theta^{-1} : \mathbf{D} \to \mathbf{G}$ is straightforward. (An optimized FORTRAN 77 package that implements the above algorithm has been written by M&M and can be obtained directly from the authors of [13].)

IV. The Gain-phase Phase Margin Problem

The gain-phase margin [14], [6] is a measure of robustness against simultaneous gain and phase perturbations. In our setting this corresponds to families of plants where

$$\mathbf{K} = \{re^{j\phi} : r \in [a, b], 0 < a < 1 < b;$$
$$\phi \in [\varphi_1, \varphi_2], -\pi < \varphi_1 \le 0 \le \varphi_2 < \pi\}. \tag{14}$$

The controller that robustly stabilizes this family will achieve a generalized gain margin of $\kappa = \sqrt{b/a}$ and generalized phase margin of $\varphi = (\varphi_2 - \varphi_1)/2$. The classical gain and phase margins are obtained by setting $a = 1/b$ and $-\varphi_1 = \varphi_2$, respectively. The domain $\mathbf{G}$ for the gain-phase margin problem the image of $\mathbf{C} \setminus \mathbf{K}$ under the mapping $\phi_S(z) = \frac{z}{z-1}$ (see Fig. 4).

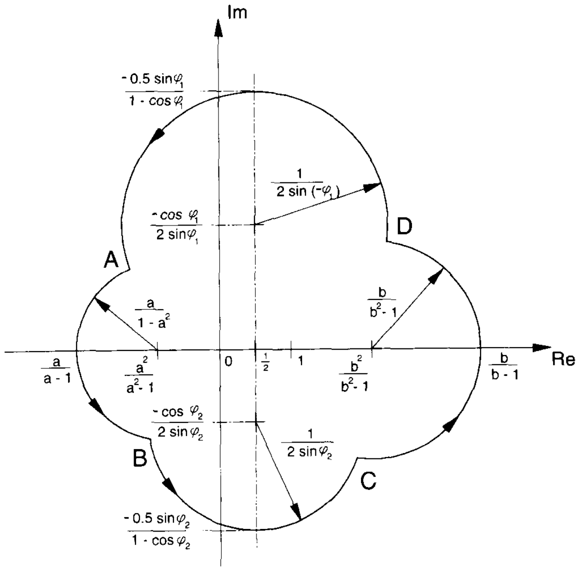

Fig. 4. Set $\mathbf{G}$ of the gain-phase margin problem.

Remark 3: The gain and phase margin problems are limiting cases of the gain-phase margin problem. In fact

$$\text{as } \varphi \to 0, \mathbf{G} \to \mathbf{C} \setminus (-\infty, \frac{a}{a-1}] \cup [\frac{b}{1-b}, \infty)$$
$$\text{as } \kappa \to 1, \mathbf{G} \to \mathbf{C} \setminus (-\infty, \frac{1}{2} - j\frac{1}{2}\frac{\sin(\varphi_2)}{1-\cos(\varphi_2)}] \cup [\frac{1}{2} + j\frac{1}{2}\frac{\sin(-\varphi_1)}{1-\cos(-\varphi_1)}, \infty).$$

Moreover, it can be shown that for the gain margin and phase margin problems

$$|\theta(1)| = \begin{cases} \frac{\kappa-1}{\kappa+1}, & \varphi = 0 \\ \sin(\varphi/2), & \kappa = 1. \end{cases} \tag{15}$$

The optimal stability margin occurs when $|\theta(1)| = \alpha_{opt}$, and we can use (15) to obtain the optimal gain margin, κ_{opt}, and phase margin, φ_{opt} in terms of α_{opt}. In the gain-phase margin problem, however, the condition $|\theta(1)| = \alpha_{opt}$ does not define a unique optimal gain-phase margin pair $(\kappa, \varphi)_{opt}$. In fact $(\kappa_{opt}, 0)$ and $(1, \varphi_{opt})$ both achieve $|\theta(1)| = \alpha_{opt}$. This is illustrated in Fig. 5 where we have plotted the gain-phase pairs corresponding to a fixed value of α_{opt}. This extra freedom can be used to choose the optimal gain-phase margin most convenient to our applications. For example, define a gain-phase ratio $\beta(\kappa, \varphi)$ as: $\beta(\kappa, \varphi) = (1 - \kappa^{-1})\varphi$ and set $\beta_{opt} = \beta(\kappa_{opt}, \varphi_{opt})$. Then, the optimal gain-phase margin $(\kappa, \varphi)_{opt}$ is determined by the intersection of the curves $\beta(\kappa, \varphi) = \beta_{opt}$ and $|\theta(1)| = \alpha_{opt}$. Thus, we can define the optimal gain-phase margin as follows.

Definition 1: Let $\beta_{opt} := \beta(\kappa_{opt}, \varphi_{opt})$ be the optimal gain-phase ratio where $\beta(\kappa, \varphi)$ is a suitable gain-phase ratio function. The optimal gain-phase margin is the pair $(\kappa, \varphi)_{opt}$ such that $\beta(\kappa, \varphi) = \beta_{opt}$ and $|\theta(1)| = \alpha_{opt}$.

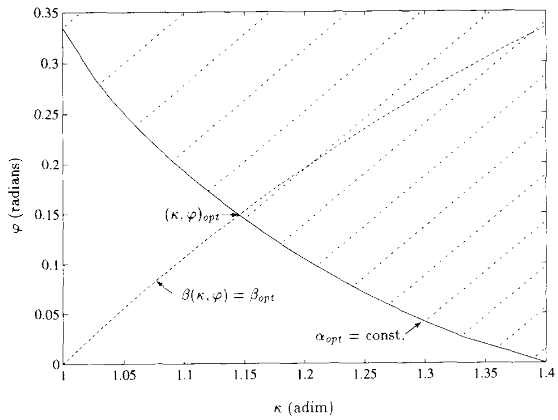

Fig. 5. Defining the optimal gain-phase margin.

V. Examples

Let $P_o(s) = \frac{(s+1)(s-5)}{(s-1)(s-3)}$. We want to compute the optimal gain-phase margin and a strictly proper controller that maximizes such margin. In addition we want the closed loop to reject step disturbances. The unstable zeros and poles of P_o are $z = \{5\}$ and $p = 1, 3$, respectively. We have also interpolation conditions at the boundary: one at $s = \infty$ (strictly proper compensator) and one at $s = 0$ (integral action), thus $S_o(a_i) = b_i$, where $\mathbf{a} = [0, 1, 3, 5, \infty]$, $\mathbf{b} = [0, 0, 0, 1, 1]$. From $\mathbf{a}$ and $\mathbf{b}$ we compute $\alpha_{opt} = 1/6$. For this value of α_{opt} we have $\kappa_{opt} = 1.4$ (2.9 dB) and $\varphi_{opt} = 0.3349$ rad. (19.1 degrees). The combined optimal gain-phase margin is $(1.12$ dB, 8.52 deg.$)_{opt}$. It is computed via binary search. The next step is to find $C = P_o^{-1}[S_o^{-1} - 1]$, where $S_o = \theta^{-1}(\tilde{S})$. Due to interpolation conditions at the boundary α_{opt} cannot be achieved, so we settle for a suboptimal solution with $\alpha < \alpha_{opt}$. Let $\alpha = 1/8.4$. We first find $\tilde{S}_o$ by solving a NP problem with data $\mathbf{a} = [0, 1, 3, 5, \infty]$, $\mathbf{b} = [0, 0, 0, 8.4^{-1}, 8.4^{-1}]$. A solution (not unique) is

$$\tilde{S}_o(s) = \frac{1}{8.4} \times \frac{s^4 + 125.5s^3 - 515.0s^2 - 388.5s}{s^4 + 20.50s^3 + 73.58s^2 + 67.80s + 13.72}.$$

We then compute $S_o(j\omega) = \theta^{-1}(\tilde{S}(j\omega))$ and recover $S_o(s)$ using the GKL rational approximation algorithm [15]. Finally we obtain the equation found at the bottom of the page. The high order of the controller is due to the shape of the gain-phase region $\mathbf{G}$. This behavior is characteristic of uniform optimization methods where the order of the controller is intimately related to the performance specifications, in this case represented by $\mathbf{G}$.

VI. Conclusions

Many problems of robust stabilization can be reduced to interpolation problems via conformal mappings. These conformal mappings are difficult to find analytically and must be constructed numerically. Here we have presented a new numerical algorithm to construct such conformal mappings. We have also demonstrated its application to the synthesis of optimal stability margin controllers, in particular, for

$$C(s) = \frac{-1.06e2s^{13} - 2.139e3s^{12} - 2.760e4s^{11} - 1.967e5s^{10} - 1.022e6s^9 - 3.321e6s^8 - 7.595e6s^7}{s^{13} + 1.517e2s^{12} + 3.107e3s^{11} + 4.038e4s^{10} + 3.102e5s^9 + 1.718e6s^8 + 6.444e6s^7}$$
$$\cdots \frac{-1.241e7s^6 - 1.123e7s^5 - 4.670e6s^4 + 1.481e6s^3 + 2.858e6s^2 + 9.692e5s - 5.296e4}{+1.783e7s^6 + 3.573e7s^5 + 5.012e7s^4 + 4.874e7s^3 + 3.202e7s^2 + 1.288e7s + 2.371e6}$$

the gain-phase margin problem. To apply this approach to more general robust stabilization problems, a frequency dependent conformal mapping must be constructed. This problem as well as its extension to multivariable systems are subjects of ongoing research.

References

[1] P. Khargonekar and A. Tannenbaum, "Non-euclidean metrics and the robust stabilization of systems with parameter uncertainty," *IEEE Trans. Automat. Contr.*, vol. 30, no. 10, pp. 1005–1013, Oct. 1985.

[2] A. Tannenbaum, *Invariance and System Theory: Algebraic and Geometric Aspects*. New York: Springer-Verlag, 1981.

[3] ——, "Modified Nevanlinna–Pick interpolation and feedback stabilization of linear plants with uncertainty in the gain factor," *Int. J. Contr.*, vol. 36, pp. 331–336, 1982.

[4] W. Y. Yan and B. D. O. Anderson, "The combined sensitivity and phase margin problem," *Automatica*, vol. 28, no. 2, pp. 417–422, Mar. 1992.

[5] A. W. Olbrot and M. Nikodem, "Robust stabilization: Some extensions of the gain margin maximization problem," *IEEE Trans. Automat. Contr.*, vol. 39, no. 3, pp. 652–657, Mar. 1994.

[6] J. C. Cockburn, Y. Sidar, and A. Tannenbaum, "A constructive solution to the gain-phase margin problem," in *IEEE Proc. 31st CDC*, vol. 1, Dec. 1992, pp. 682–683.

[7] A. Sideris, "Robust feedback synthesis via conformal mappings and H^∞ optimization," Ph.D. dissertation, Univ. Southern California, July 1985.

[8] J. Doyle, B. Francis, and A. Tannenbaum, *Feedback Control Theory*. New York: MacMillan, 1992.

[9] J. L. Walsh, *Interpolation and Approximation by Rational Functions in the Complex Domain*, (AMS Colloquium Pub.), 4th ed., vol. 20. Providence, RI: AMS, 1965.

[10] J. B. Conway, *Functions of One Complex Variable*. New York: Springer-Verlag, 1978.

[11] P. Henrici, *Applied and Computational Complex Analysis*, vol. III. New York: Wiley, 1986.

[12] L. N. Trefethen, "Numerical computation of the Schwarz-Christoffel transformation," *SIAM J. Sci. Stat. Comput.*, vol. 1, pp. 82–102, Mar. 1980.

[13] D. Marshall and J. Morrow, "Unzipping plane domains," manuscript, June 1987.

[14] Y. Sidar, "The combined problem of gain and phase margins in linear control systems— theoretical boundaries using Nevanlinna–Pick interpolation theory," Master's thesis, Israel Institute of Technology, Haifa–Israel, May 1990.

[15] G. Gu, P. Khargonekar, and E. B. Lee, "Approximation of infinite-dimensional systems," *IEEE Trans. Automat. Contr.*, vol. 34, no. 6, pp. 610–618, June 1989.

Event-Averaged Maximum Likelihood Estimation and Mean-Field Theory in Multitarget Tracking

Keith Kastella

***Abstract*—This paper presents a novel type of Kalman filter for track maintenance in multitarget tracking using thresholded sensor data at high target/clutter densities and low detection levels. The filter is robust against tracking errors induced by crossing tracks, clutter, and missed detections, and the computational complexity of the filter scales well with problem size. There are two key features that differentiate this approach from earlier work. First, to reduce computational load, the filter exploits techniques from statistical field theory to simplify measurement to track association by using a mean-field approximation to sum over associations. Second, to enhance tracking of close together targets, the filter explicitly models the error correlations that occur between such target pairs. These error correlations are caused by measurement to track association ambiguities that arise when target separations are comparable to sensor measurement errors.**

I. Introduction

A typical multitarget tracking problem for a sensor such as a primary radar involves both clutter and ambiguous associations of measurements with tracks. Most algorithms approach this problem as one of statistical estimation [2], [3]. There are two subproblems that these algorithms attempt solve. First, it is not known which measurements are clutter and which are generated by targets. Second, the association of the target-originated returns with the tracks is unknown. Together, these subproblems constitute the "data association problem." These algorithms assume that the measurement to track association (MTA) must be estimated as part of the track estimation process. They proceed by computing an assignment cost or likelihood for some or all of the feasible MTA's. The individual associated measurements or some set of averages over them are then used to update independent Kalman filters (one for each track) to form updated track estimates. As target and clutter densities increase, however, the probability of correctly associating a measurement with its originating track rapidly decreases [14]. This, in turn, leads to a persistent bias in the track estimate for closely spaced tracks [5], [10], [12].

Another difficulty with multitarget tracking is that the number of possible measurement to track associations is large. With perfect detection and no false alarms, T targets will generate $T!$ possible MTA's for a single scan. This is exacerbated when false alarms are present and detection is not perfect. In practice, it is possible to factorize the problem into collections of noninteracting clusters of targets. The relevant parameter T is then the number of targets in the largest typical such cluster. This can be large, especially if passive sensors providing no range data are used.

To address these issues, we have developed a new approach to multitarget tracking based on event-averaged maximum likelihood estimation (EAMLE) [13]. Unlike the conventional view that data association is central to multitarget tracking, EAMLE does not require computing the MTA likelihood to form track estimates. Since the sensor provides no information about the correct MTA, the average

Manuscript received April 5, 1994; revised November 17, 1994. This work was supported in part by Air Force Office of Scientific Research Contract AFOSR/F49620-94-1-0275.

The author is with UNISYS Government Systems Corporation, St. Paul, MN 55164-0525 USA.

IEEE Log Number 9409692.

0018–9286/95$04.00